QUANTUM SIMULATIONS READING PROJECT

Mahadevan Subramanian, Undergraduate at Department of Physics, IIT Bombay

Guide: Professor Alok Shukla, Department of Physics, IIT Bombay

Contents

ABSTRACT

Quantum simulation is a very interesting problem, while hard in nature to implement on classical computers one can find efficient ways to implement them in certain cases using quantum systems. Here we aim to explore algorithms for the execution of Hartree-Fock methods, configuration interactions, and coupled-cluster type calculations on quantum computers.

1 Review on Quantum Simulation

This section is made with reference to [3].

1.1 Introduction

The problem of creating a simulation of a quantum system is a famous and very difficult task. If one were to make use of a classical computer the resources required would scale exponentially. For example if one were to store a state of N spin 1/2 particles we would need to store 2^N numbers for the state and 4^N for the unitary evolution (this is about 4TB for $N = 40$).
There do exist certain classical stochastic methods which can be used for certain systems (specifically those where the functions being integrated do not change sign and vary slowly). The Quantum Monte Carlo methods offer a polynomial time implementation for the quantum many body simulation.
One of the alternatives to simulate quantum systems was proposed by Feynman. Bluntly put we use quantum systems

to simulate quantum systems. The method described uses a mapping of the desired state and desired evolution to a state of the system and it's evolution. We denote the system state by $|\varphi\rangle$ and it goes from $|\varphi(0)\rangle$ to $|\varphi(t)\rangle$ with evolution $U = \exp(-\iota\hbar H_{sys}t)$. The simulator state $|\psi\rangle$ goes from $|\psi(0)\rangle$ to $|\psi(t)\rangle$ with evolution $U^{'} = \exp(-\iota\hbar H_{sim}t)$. If we can create a mapping between the final and initial states and the evolution operator, we can simulate this system.

1.2 Digital and Analog Quantum Simulations

1.2.1 Digital Quantum Simulation

Here we make use of qubits for simulating the systems. Suppose we want to simulate spin 1/2 particles, we assign each particle to one qubit and we prepare our simulator state $|\psi(0)\rangle$ using the 1,0 convention for spin up and down respectively. For getting $|\psi(t)\rangle = \exp(-\iota\hbar Ht)\,|\psi(0)\rangle$ we apply the unitary $U = \exp(-\iota\hbar Ht)$ to our initial state by decomposing it into single qubit and two qubit gates (eg: U3 and CNOT gates are universal). This is referred to as DQS (digital quantum simulation) and since we can make a circuit for all unitaries, DQS is universal however we need not be able to find an efficient decomposition for all unitaries.
State preparation in general is a task which need not be efficient but in some cases there are convenient efficient algorithm. For example there is an algorithm for efficiently preparing a state of m electrons occupying n orbitals using recursion to reverse engineer the given state to the $|0\rangle^{\otimes(n)}$
For the actual evolution of state we use the Trotter's formula for dealing with systems of form $H = \sum_{i=1}^{n} H_i$ by using the fact that $\lim_{n\to\infty}(\prod_i \exp(H_i/N))^N = \exp(\sum_i H_i)$ since all the commutation terms are second order with $1/N$ hence in the limit go to zero so we break our unitary into small time steps to make sure that the error doesn't go large. The algorithms functions like this (reference: [7])
Inputs: The initial state $|\psi_0\rangle$ along with the Hamiltonian $H = \sum_{k=1}^{L} H_k$, the error range δ and time t_f for which we have to find $|\psi(t_f)\rangle$. Here $U_{\Delta t} = \prod_{k=1}^{L} \exp(-\iota\hbar H_k \Delta t)$
Outputs: The state $|\psi(\tilde{t}_f)\rangle$ such that $|\,\langle\psi(\tilde{t}_f)|\,|^2 < 1 - \delta$
Procedure:

1. Initialize state as $|\tilde{\psi_0}\rangle = |\psi_0\rangle$.
2. Iterative update $|\psi_{j+1}\rangle = U_{\Delta t}\,|\psi_j\rangle$.
3. $j = j + 1$; goto 2. while $j\Delta t < t_f$.
4. $|\psi(\tilde{t}_f)\rangle = |\tilde{\psi_j}\rangle$ final result

Runtime: This typically functions in $O(poly(1/\delta))$ operations. Here $U_{\Delta t}$ is a unitary which describes the approximate evolution over a time of Δt
Now comes the process of measurement. Generally for quantum systems this is done via quantum state tomography however those require resources that scale exponentially with the size of the system. To get around this estimation is done of correlation functions or spectra of operators.

1.2.2 Analog Quantum Simulation

In analog quantum simulation a real quantum system is used to simulate another quantum system and the real quantum system would be controllable hence one can make inferences about the simulated system using this possibly easier to control system by using mappings. The mappings are made as $H_{sim} = fH_{sys}f^{-1}$ where the initial state is transformed using f and we get the final state by transforming back with f^{-1}. Essentially we must note that H_{sim} and H_{sys} have the same eigenvalues for this to be a valid mapping. An example of hamiltonians like this would be a hamiltonian describing a gas of interacting bosonic atoms in a periodic potential and the Bose-Hubbard hamiltonian.

$$H_{sim} = -J\sum_{i,j}\hat{a}_i^\dagger\hat{a}_j + \sum_i \epsilon_i\hat{n}_i + \frac{1}{2}\sum_i \hat{n}_i(\hat{n}_i - 1) \tag{1}$$

$$H_{BH} = -J\sum_{i,j}\hat{b}_i^\dagger\hat{b}_j - \mu\sum_i \hat{n}_i + \frac{1}{2}\sum_i \hat{n}_i(\hat{n}_i - 1) \tag{2}$$

The bosonic atoms hamiltonian is described in 1 where $\hat{a}_j$ and $\hat{a}_j^\dagger$ are the bosonic annihilation and creation operators respectively and J is the hopping strength and U is the interaction strength. ϵ_i represents the energy offset. One can see that eq1 is quite similar to eq2. The μ eq2 is the chemical potential and that is pretty much the only difference. One can execute the Bose-Hubbard hamiltonian as described by eq2 using atoms in an optical potential. However

there need not be a straightforward mapping in most situations. AQS does have quite some advantages over DQS such as the fact that state preparation would occur naturally as the system would naturally gravitate toward the equilibrium state normally. Also measurement can be done directly unlike the computational manipulation required in DQS.

1.3 Resource estimation

There is a general rule of thumb that to outperform a normal computer with a quantum computer one would need somewhere between 40 to 100 qubits. There are plenty of interesting things that can be done with about 10 qubits too from proof of concept simulations to even quantum chaos. However when you only need a few qubits you might as well use a classical computer. In DQS the estimate for representing N particles with pairwise potential would require n qubits for representing the wave function as a discrete variable and we would need m qubits for estimation of values to some precision. The Coulomb potential can be calculated in $\mathcal{O}(N^2m^2)$ steps which is clearly an exponential improvement from the classical way of calculation. There is however an overhead cost in for the gates as the step size decreases in trotterization.
It is stated that AQS has less stringent resource requirements and can proceed useful results with classical computers. In AQS one can manipulate a larger number of particles with more resources for example hundreds of thousands of atoms have been trapped using only three laser beams.
In AQS effects of decoherence are generally believed to be less dramatic and is even suggested that it might be useful as a way of modelling decoherence of the simulated system. If the noise level naturally present in the simulator is lower than the simulated system one can artificially supplement the noise so that it faithfully mimics the simulated system. In principle one can make use of the natural symmetries present in the system so as to modify the effective decoherence using appropriate mappings. There are cases where fault tolerant methods are inefficient compare to trotter approximation such as finding the low lying spectrum of a pairing hamiltonian in an NMR implementation. Two qubit entanglement was found to be exponentially sensitive to both small changes in the hamiltonian and locations of the chosen qubits due to natural ordering introduced on the qubits by coding of the simulated system.

1.4 Physical Realizations

All physical systems that can be used as a quantum computer would also be a universal machine for DQS. However there are various quantum systems that can be used to implement AQS.

1.4.1 Atoms and Ions

Neutral atoms in optical lattices are well suited to mimic solid state systems. These optical potentials can be adjusted to change geometry and dimensionality of lattice like creating triangular or Kagome lattices. These are quite flexible systems where there are several controllable parameters and there are both bosonic and fermionic elements that can be used here. A general Hubbard hamiltonian is written as

$$H = H_{hop} + H_{interaction} + H_{pot} + H_{internal} \tag{3}$$

One can simulate the Mott insulator-superfluid phase transition using this system by tuning the on-site interactions using Fresbach resonances. Continuous tunability of interaction strength allows one to enter a regime called the unitary regime where interaction strength is comparable to Fermi energy so we only have one energy scale in our system. Addressing individual atoms is a tough task however due to the best laser focusing widths are typically near the scale of lattice distance $(0.5 - 0.8\mu m)$
One can even use these for DQS since one can make controlled operations by using a double optical potential with interaction between neighbouring atoms.
Using ions one can make multiple qubit gates by making use of their Coulomb repulsion and ion qubits tend to have much longer coherence times (in the order of seconds) and can also make sequences of high fidelity quantum gates.
The quantum states for trapped ions are mostly manipulated using resonantly driving transitions between internal states of the ions or resonantly driving sideband transitions involving the internal states and vibrational states of the ions in the trapping potential. The hamiltonian describing coupling between internal and vibrational modes due to laser driving at red-sideband frequency is the following

$$H = \iota\hbar\eta\Omega[\exp(\iota\varphi)\sigma_+ a - \exp(-\iota\varphi)\sigma_- a^\dagger] \tag{4}$$

Here Ω is the Rabi frequency of transition between the internal states, σ_+ and σ_- are the two level atom transition operators. $a, a^\dagger$ are the ladder operators for the vibrational modes and ϕ is laser phase and η is the Lambe-Dicke parameter. Using this one can realize quantum gates for DQS and even some hamiltonians for AQS. High fidelity one,two,three qubit (toffoli) gates have been implemented using this. Ions have generally been trapped using linear harmonic traps.

1.4.2 Nuclear and electronic spins

Nuclear spin qubits have long coherence times ($> 1s$) and high fidelity quantum gates of up to 12 qubits have been demonstrated. Here nuclear spins are manipulated using NMR (nuclear magnetic resonance). The general form of the hamiltonian is

$$H = -\hbar\gamma B \sum_i I_i^z + \sum_{i>j} J_{ij} I_i^z I_j^z \tag{5}$$

Here I is the angular momentum operator and J represents the spin-spin coupling coefficients. B is magnetic field and γ is the gyro-magnetic ratio. The different transitions between pairs of energy levels generally have distinct resonance frequencies which makes it possible to implement multi qubit gates using rf (radio frequency) pulses. Scaling is however a big issue here but can be possibly addressed by making use of nitrogen vacancy centers for strongly correlated systems.
Another system that is used are electron spins in semiconductor quantum dots. Quantum dots are semiconductor systems where excitations are confined in small regions in one or two dimensions and if they are roughly as wide as the wavelength of charge carrier they sort of have quantized levels similar to those of actual atoms. Readout can be manipulated both electrically and optically. They have decay times of $> 1s$. A hamiltonian for an array of quantum dots is given by

$$H = \sum_{j=1}^{n} \mu_B g_j(t) B_j(t) \cdot S_j + \sum_{1 \le j < k \le n} J_{jk}(t) S_j \cdot S_k \tag{6}$$

The first term comes form energy of applied magnetic field and the second term is exchange interaction due to virtual tunneling between quantum dots and S_j is spin of the electric charge quanta of the jth dot.

1.4.3 Superconducting circuits

There are many ways in which one can encode quantum information in superconducting circuits: number of superconducting electrons on a small island, direction of current around a loop or in oscillatory states of the circuit. The circuit can be manipulated by applied voltages and currents. These have an advantage over real atoms since one can tailor characteristic frequencies, interaction strengths and so on much easily. Hamiltonian for N charge (flux) qubits biased at their symmetry points (optimal for quantum coherence) coupled capacitively is

$$H = -\sum_{i=1}^{N} \frac{\Delta_i}{2} \sigma_i^Z - \sum_{i,j} J_{ij} \sigma_i^Z \sigma_j^Z \tag{7}$$

Where Δ_i is level splitting and the J_{ij} is for coupling strength between i and j qubits. It must be noted that these are not two level systems however these additional levels could possibly be utilized for AQS for spin greater than 1/2.

1.4.4 Photons

Photons can carry quantum information over long distances and would hardly be affected by noise and decoherence and can encode qubits using polarization. One qubit gates can easily be realized using linear optical components however implementing two qubit gates for photonic systems are much more difficult. These have been used for many impressive tasks however like to calculate the possible fractional statistics of anyons using a six photon graph state, calculate the energy system of spectrum of hydrogen to 10 bits of precision and even simulate frustrated spin systems. These do have issues in flexibility and scalability so have a long way to go.

2 Hartree-Fock Theory

2.1 The formulae

The main aim here is calculations involving many electron systems in a pairwise potential. Using the Born-Oppenheimer approximation one can find the exact solutions for a hydrogen atom (or any one electron atom) however exact solutions cannot be found once we have more than one electron. The idea of the approximation is to consider that nuclei are relatively stationary since electron movement is much faster. Let's first write the for an N electron system with N_{nucl} nuclei each with some Z_j atomic number at $\vec{R}_j$.

$$H^{el} = \sum_{i=1}^{N} \frac{p_i^2}{2m} - \sum_{i=1}^{N} \sum_{j=1}^{N_{nucl}} \frac{Z_j e^2}{|\vec{r}_i - \vec{R}_j|} + \sum_{i>j=1}^{N} \frac{e^2}{|\vec{r}_i - \vec{r}_j|} \tag{8}$$

Our aim is to solve $H|\psi(1,2,\ldots,N)\rangle = E|\psi(1,2,\ldots,N)\rangle$. We must note that this will be anti symmetric since it describes fermions. We will adopt the mean field approach where we assume particle's dynamics are decided by a mean field created by particles at rest. Another assumption is that each electron is described by a single electron wavefunction called the spin orbital which we represent as $\phi_i(x)$ which has both a spatial and spin component. The final solution is represented as a determinant called the slater determinant

$$\psi(\vec{x}_1,\vec{x}_2,\ldots,\vec{x}_N) = \frac{1}{\sqrt{N!}}\begin{bmatrix}\phi_1(x_1) & \phi_1(x_2) & \ldots & \phi_1(x_N)\\ \phi_2(x_1) & \phi_2(x_2) & \ldots & \phi_2(x_N)\\ \vdots & \vdots & \ddots & \vdots\\ \phi_N(x_1) & \phi_N(x_2) & \ldots & \phi_N(x_N)\end{bmatrix} \tag{9}$$

The electrostatic potential felt by an electron occupying orbital $\phi_i(\vec{r})$ due to the mean field of remaining $N-1$ electrons would be

$$V_i(\vec{r}) = \sum_{j=1,j\neq i}^{N} \langle\phi_j| \frac{e^2}{|\vec{r}-\vec{r'}|} |\phi_j\rangle \tag{10}$$

We also will define $V_{nucl}(\vec{r})$ which is the nuclear attraction potential felt by an electron at $\vec{r}$ then we have

$$V_{nucl}(\vec{r}) = \sum_{i=1}^{N_{nucl}} \frac{Z_i e^2}{|\vec{r}-\vec{R}_i|} \tag{11}$$

From this we get the Hartree equation

$$\left(-\frac{\hbar^2}{2m}\nabla^2 + V_{nucl}(\vec{r}) + V_i(\vec{r})\right).\phi_i(\vec{x}) = \varepsilon_i\phi_i(\vec{x}) \tag{12}$$

Clearly the nuclear attraction potential is a one eletron operator and the electrostatic potential is a two electron operator. The following equation shows the expectation values for one electron and two electron operators.

$$\langle\Phi| O_1 |\Phi\rangle = \sum_i \langle\phi_i| f |\phi_i\rangle = f_{ii}, O_1 = \sum_i f(\vec{r}_i) \tag{13}$$

$$\langle\Phi| O_2 |\Phi\rangle = \frac{1}{2}\sum_j\sum_i(\langle\phi_i\phi_j| g |\phi_i\phi_j\rangle - \langle\phi_i\phi_j| g |\phi_j\phi_i\rangle), O_1 = \sum_{i,j} g(\vec{r}_i) \tag{14}$$

So the whole thing is reduced into an eigenvalue problem. We define the operators $h(\vec{r}_i) = \frac{p_i^2}{2m} + V_{nucl}(\vec{r}_i)$, $V_H|\phi_i\rangle = \sum_{j=1}^N \langle\phi_j| \frac{e^2}{r_{12}} |\phi_j\rangle |\phi_i\rangle$, $V_{ex}|\phi_i\rangle = \sum_{j=1}^N \langle\phi_j| \frac{e^2}{r_{12}} |\phi_i\rangle |\phi_j\rangle$ and the problem reduces to the following eigenvalue problem

$$(h + V_H + V_{ex})|\phi_i\rangle = \varepsilon_i|\phi_i\rangle \tag{15}$$

The total energy however is not simply the sum of all the orbital energies for the system and is actually $E_{HF} = \frac{1}{2}\sum_{i=1}^N(\varepsilon_i + h_{ii})$. We call the fock operator as $F = h + V_H + V_{ex}$.

2.2 Canonical transformations

This part is made with reference to supplementary materials provided in [1]. For solving the hartree fock equations and arriving at the asymmetric state the state is variationally solved such that energy is stationary with respect to first order changes in the wavefunction and we start from an arbitrary orthogonal basis $\{\phi_i\}$. So we solve $\langle\delta\psi| H|\psi\rangle = 0$. We assume the solution is represented as

$$\langle r|\psi\rangle = \langle r|\prod_{i=1}^{n} a_i^\dagger |vac\rangle = \frac{1}{\sqrt{n!}}\det\begin{bmatrix}\chi_1(r_1) & \ldots & \chi_1(r_n)\\ \vdots & \ddots & \vdots\\ \chi_n(r_1) & \ldots & \chi_n(r_n)\end{bmatrix} \tag{16}$$

We will now index the states which are in the product wavefunction by i and those which aren't by a. We then can write the first order variation as $\langle\delta\psi| = \langle\psi| a_i^\dagger a_a\zeta$ where ζ is the first order variation in χ_i so we get the expression for the stationarity of the state as

$$\langle\psi| a_i^\dagger a_a H|\psi\rangle = 0 \tag{17}$$

We also have the one-body fermionic generators form a closed lie-algebra

$$[a_p^\dagger a_q, a_r^\dagger a_s] = \delta_{q,r} a_p^\dagger a_s - \delta_{p,s} a_r^\dagger a_s \tag{18}$$

The adjoint representation of an element of the algebra would be $\kappa = \sum_{p,q} \kappa_{p,q} a_p^\dagger a_q$ and it's commutators can be represented as $[\kappa, a_p^\dagger] = a_p^\dagger \kappa_{p,q}$ and $[\kappa, a_p] = a_p \kappa_{p,q}^*$. We then define similarity transformations on the ladder operators: $e^K a_p^\dagger e^{-K} = \sum_q a_q^\dagger u_{q,p}$, $e^K a_p e^{-K} = \sum_q a_q u_{q,p}^*$ and here u is the matrix given by the exponentiation of the coefficient matrix for the generator operator κ so it is $u = e^\kappa$.
Any rotation of the underlying basis can now be written with the similarity transform as

$$|\phi(\kappa)\rangle = e^K a_1^\dagger e^{-K} \dots e^K a_n^\dagger e^{-K} = e^K |\psi\rangle \tag{19}$$

Now before we proceed we must note that the 2-RDM (reduced density matrix) can be obtained from the 1-RDM since

$$^1D_i^j = \langle\phi| a_j^\dagger a_i |\phi\rangle \tag{20}$$

$$^2D_{ij}^{pq} = \langle\phi| a_p^\dagger a_q^\dagger a_j a_i |\phi\rangle = {}^1D_i^{p\,1}D_j^q - {}^1D_i^{q\,1}D_j^p \tag{21}$$

Using expression of energy we get that we can express energy in terms of the 1-RDM purely since we can write the 2-RDM in terms of 1-RDM.

$$E(\kappa) = \sum_{ij} h_{ij} \langle\phi(\kappa)| a_i^\dagger a_j |\phi(\kappa)\rangle + \sum_{ijkl} V_{ijkl} \langle\phi| a_i^\dagger a_j^\dagger a_k a_l |\phi\rangle \tag{22}$$

$$= \sum_{ij} h_{ij} {}^1D_i^j + \sum_{ijkl} V_{ijkl} {}^2D_{lk}^{ij} \tag{23}$$

3 Simulation of H_2 molecule using chloroform

This section is essentially a summary of the ideas discussed in [2]. The paper shows results of calculation of ground state of a hydrogen molecule which as done to 45 bits of accuracy in 15 iterations. The main idea of the calculation is that the ground state is prepared using adiabatic state preparation and then phase estimation of eigen value is done but instead of using the inverse fourier transform method, an iterative NMR interferometer is used. It must be noted that to obtain a 45 bit accuracy in the phase value one would require 45 qubits in the register that is used for phase measurement using the inverse QFT method if one wants to extract the whole information with one circuit.

3.1 Phase estimation using QFT

This is just a description of how phase estimation is done using the quantum fourier transform normally taken from [7]. Suppose we have unitary operator U with an eigen vector $|u\rangle$ with an eigenvalue $e^{2\pi\phi}$ where ϕ is unknown and we wish to estimate its value. We us two registers, one which has t qubits and the other which is initialized in state $|u\rangle$. Now lets say that the binary representation of ϕ is $0.\phi_1\phi_2...\phi_t$ accurate to t places after the radix point.
The state of the first register will now be

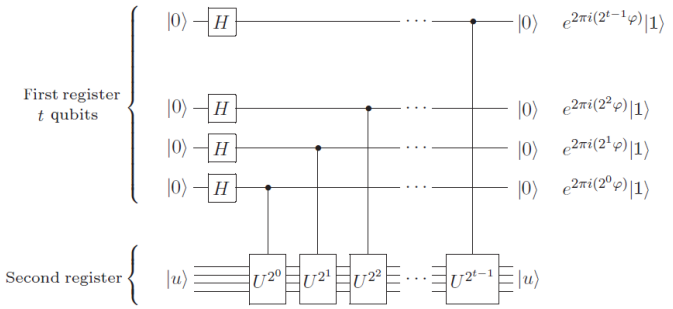

Figure 1: Circuit for phase estimation. Note that we perform inverse Fourier transform on the first register and then a measurement on the first register

$$\frac{(|0\rangle + e^{2\pi\iota 0.\phi_t}|1\rangle)(|0\rangle + e^{2\pi\iota 0.\phi_{n-1}\phi_n}|1\rangle).....(|0\rangle + e^{2\pi\iota 0.\phi_1\phi_2...\phi_n}|1\rangle)}{2^{n/2}}$$

Clearly doing an inverse Fourier transform over this will give us the state $|\phi_1\phi_2...\phi_t\rangle$ hence on measurement we will be able to estimate this phase.

3.2 Description of the system

The hamiltonian of the hydrogen molecule can be described by the following equation

$$H = \sum_{i=1}^{2}(T_i + \sum_{j=1}^{2} V_{ij}) + \sum_{i,j=1,i>j}^{2} O_{ij} \tag{24}$$

Here T_i is the kinetic energy of the ith electron and V_{ij} is the Coulomb potential energy between the ith electron and the jth nucleus and O_{ij} is the Coulomb potential energy between the ith and jth electron. This is under the Born Oppenheimer approximation where the nuclei are assumed at rest.
This molecule has two nuclei and two electrons and the two 1s orbitals can combine to form a gerade bonding orbital and an ungerade antibonding orbital 4 spin orbitals which can be occupied hence giving 6 possible configurations (4 choose 2). The only two states we will be concerned with are the ground state $|\Psi_0\rangle$ and the double excited state $|\Psi_{11}^{22}\rangle$ giving us the following hamiltonian matrix which has a theoretical eigen value of -1.851 570 929 351 19 a.u.

$$\mathcal{H} = \begin{pmatrix} \langle\Psi_0| H |\Psi_0\rangle & \langle\Psi_0| H |\Psi_{11}^{22}\rangle \\ \langle\Psi_{11}^{22}| H |\Psi_0\rangle & \langle\Psi_{11}^{22}| H |\Psi_{11}^{22}\rangle \end{pmatrix} = \begin{pmatrix} -1.8310 & 0.1813 \\ 0.1813 & -0.2537 \end{pmatrix}$$

When doing the experimental implementation chloroform ($CHCl_3$) with carbon-13 dissolved in d_6 acetone as a two qubit computer where ^{13}C nulceus is used for the system qubit and the H atom is used for probe qubit. The natural hamiltonian of the system is the following

$$\mathcal{H}_{\text{NMR}} = \frac{\omega_p}{2}\sigma_z^p + \frac{\omega_s}{2}\sigma_z^s + \frac{\pi J_{ps}}{2}\sigma_z^p\sigma_z^s$$

Here J_{ps} represents the coupling constant and is typically 214.6 Hz in value. The $\omega_s/2\pi$ and $\omega_p/2\pi$ are the Larmor frequencies.

3.3 Calculation of the ground state energy

The first step is creation of ground state of $\mathcal{H}$ in the system qubit. It is essentially done by applying three pulses of rotations $R_x(\theta_3)R_{-y}(\theta_2)R_{-x}(\theta_1)$ in multiple steps. In the ASP process we start with an initial hamiltonian of $H_0 = \sigma_x$ and is prepared at it's ground state of $|-\rangle$. This is then driven to the actual system hamiltonian $\mathcal{H}$ using linear interpolation $H_{ad} = (1 - \frac{t}{T})H_0 + \frac{t}{T}\mathcal{H}$ and the t goes from 0 to T and so $|\Psi\rangle$ the ground state is approached as time passes. The total evolution time is taken as $T = 5.52$ a.u. to ensure success of ASP
The probe qubit is kept at the $|+\rangle$ state initially and is used as a controlled qubit for applying the U_k operator which starts as $U_0 = U$. The iterative process is done as $U_{k+1} = [e^{-\iota 2\pi\phi'_k}U_k]^{2^n}$, ϕ'_k =max$\{\phi_k - \phi_{\text{errbd}}, 0\}$ where ϕ_k is the phase shift measured in the kth iteration. In each iteration the phase shift caused by U_k is measured and here n is the number of bits extracted in each iteration and we have $2^{-n} \geq 2\phi_{\text{errbd}}$. Essentially each iteration for the given setup increases the accuracy by 3 bits.
The controlled U_k is essentially the operation $\mathcal{U}_k = |\uparrow\rangle\langle\uparrow| \otimes I + |\downarrow\rangle\langle\downarrow| \otimes U_k$. Applying this on $|+\rangle|\Psi_{asp}\rangle$ gives us $\frac{1}{\sqrt{2}}(|\uparrow\rangle + e^{\iota 2\pi\phi}|\downarrow\rangle)|\Psi_{asp}\rangle$. In an interferometer this phase shift will be seen as a relative phase between "two paths" of the $|0\rangle$ and $|1\rangle$ states hence is read out directly in NMR. Here $\phi = -E\tau/2\pi$ essentially and since one can choose any τ it is taken as $\tau = \pi/\sqrt{(2H(1,2))^2 + (H(1,1) - H(2,2))^2}$ for convenience since there is a constant α which is length of one of the pulses used in implementing the U_k operation which becomes $8^{k-1}\pi/2$ with this choice of τ.
For measurement one can measure the NMR signal of the probe qubit which is essentially just phase detection and gives us the fourier transformed spectrum of relative phase information. Each iteration would have some phase measurement and to get the actual phase value the iterative equations are used. $\phi^c_{i-1} = \phi^c_i/\phi_{\text{errbd}} + \phi'_{i-1}$ is the recursive relation and we use $\phi^c_k = \phi_k$ where ϕ_k is the measured phase of the kth iteration and we get the result that $\phi_{\text{exp}} = \phi^c_0$

3.4 Conclusions

The main takeaway from this paper was that without using the traditional setup for a phase measurement using inverse fourier transform, an iterative setup which uses NMR interferometer readings can provide a highly accurate answer

with a much smaller setup. A thing to note however which is a problem here is that implementation of the U_k gates is possible using a pulse sequence for this small scale but in general for U^j where j is fairly large would be done by j successive U implementations instead of finding a suitable pulse sequence hence resulting in cascading of errors. One possible work around which can be slightly favorable is to find pulse sequences for a good number of U^{2^n} (possibly by an algorithm specifically for this) and then for U^j we just use the binary implementation which puts a cap of $\mathcal{O}(\log_2(j))$ in size but finding the sequences should be efficient.

4 Hardware efficient VQE for small molecules and quantum magnets

This section is a summary of the ideas discussed in [4] which discusses a hardware efficient variational quantum eigensolver for finding ground states of some systems such as molecules as large as BeH_2 and for an antiferromagnetic Heisenberg model in an external magnetic field and does so using a stochastic optimization routine to create ground states.

4.1 Variational Quantum Eigensolver

Variational quantum eigensolvers are used for minimization of eigenvalue obtained from a certain state which would in fact be it's ground state. The circuit is usually set to a certain depth say d with n qubits (See figures below). RyRz has $n \times (d+1) \times 2$ parameters, Ry with linear entanglement has $2n \times (d + \frac{1}{2})$ parameters, and Ry with full entanglement has $d \times n \times \frac{(n+1)}{2} + n$ parameters. Over a certain number of iterations, these parameters are varied so as to minimize

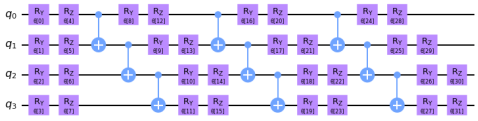

Figure 2: Circuit for linear entanglement

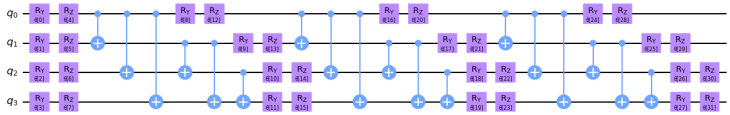

Figure 3: Circuit for full entanglement

the expectation value of the Hamiltonian $\langle\psi| H |\psi\rangle$. One can argue that this approach need not be universal since one makes a different circuit as per value of depth and that would be true since arbitrary state preparation would require a calculated approach most of the times and are proven to be efficient for some select cases (discussed in [3]).
The circuit used in [4] essentially makes the state as the following

$$|\Phi(\theta)\rangle = \prod_{q=1}^{N}[U^{q,d}(\theta)] \times U_{ENT} \times \prod_{q=1}^{N}[U^{q,d-1}(\theta)] \times \cdots \times U_{ENT} \times \prod_{q=1}^{N}[U^{q,0}(\theta)] \,|00\ldots0\rangle \tag{25}$$

Here $U^{q,i}(\theta)$ is a single qubit Euler rotation of $Z-X-Z$ applied on the q qubit at a depth of i. Here U_{ENT} is used to give entanglement and can be seen as the sequence of CNOT gates on the above figures for linear and full entanglement respectively but in case of this paper it was chosen as cross resonance gates. Z rotations were implemented as frame changes and X rotations were implemented by appropriately scaling of calibrated X_π pulses using a fixed total time of 100 ns for every single qubit rotation.
The algorithm can be written as follows:

1:	Map the quantum Hamiltonian to a qubit Hamiltonian H
2:	Set d as depth of circuit for trial state preparation
3:	Choose a set of θ_i as parameters which are for rotations applied
4:	Choose a number of samples S for the feedback loop and one S_f for final estimation
5:	Choose the maximal number of control updates k_L
6:	**while** E_f has not converged, **do:**
7:	**procedure** Quantum feedback loop:
8:	**for** $k = 1$ to k_L, **do:**
9:	Prepare trial states using θ_k and evaluate $\langle H \rangle$ with S samples
10:	Update and store the controls θ_k
11:	**end for**
12:	Evaluate $E_f = \langle H \rangle$ with S_f samples using the best controls
13:	**end procedure**
14:	Increase d, k_L, S, S_f
15:	**end while**
16:	**return** E_f

In line 9: and 10: the choice used for getting values of the new θ_k is done using optimization by gradient descent. The paper uses a simultaneous perturbation stochastic approximation (SPSA) which has also been used in context of quantum control and quantum tomography recently. In the SPSA approach at every step k, p symmetrical Bernoulli distributions Δ_k are sampled and c_k and a_k are chosen from already decided sequences that converge to zero. The gradient is evaluated as $g_k(\theta_k)$ using this

$$g_k(\theta_k) = \frac{\langle \Phi(\theta_k^+)| H |\Phi(\theta_k^+)\rangle - \langle \Phi(\theta_k^-)| H |\Phi(\theta_k^-)\rangle}{2c_k}\Delta_k \tag{26}$$

Here $\theta_k^{\pm} = \theta_k \pm c_k\Delta_k$. We then update $\theta_{k+1} = \theta_k - a_k g_k(\theta_k)$. The convergence to the optimal solution can be proven if the starting point lies in the domain of attraction however if not then convergence is not guaranteed and also in case of multiple attraction points there would be issues. The sequences chosen in this paper were

$$c_k = \frac{c}{k^{\gamma}},\ a_k = \frac{a}{k^{\alpha}}$$

with parameters $\{\alpha, \gamma\} = \{0.602, 0.101\}$ to ensure a smooth descent. The choice for c is decided based on magnitude of energy fluctuations with the θ_k since larger energy fluctuations require a larger c_k so that they do not affect gradient approximations as much. For this $c = 0.1$ is chosen for realistic simulations and $c = 0.01$ is chosen for numerical optimizations where energy is evaluated without fluctuations. The value for a is chosen so that there is a reasonable angle update in the first step since it's essentially like learning rate and so it is chosen so that the angle update is at least $2\pi/10$ and hence

$$a = \frac{2\pi}{5}\frac{c}{\left\langle \left| \langle \Phi(\theta_k^+)| H |\Phi(\theta_k^+)\rangle - \langle \Phi(\theta_k^-)| H |\Phi(\theta_k^-)\rangle \right| \right\rangle_{\Delta_1}}$$

And here the $\langle\rangle_{\Delta_1}$ means averaging over the Δ_1 distribution.

4.2 Finding the ground state energy for certain molecules

For the fermionic systems of molecules the hamiltonian can be written as

$$H = H_1 + H_2 = \sum_{\alpha,\beta=1}^{M} t_{\alpha\beta} a_\alpha^\dagger a_\beta + \frac{1}{2}\sum_{\alpha,\beta,\gamma,\delta=1}^{M} u_{\alpha\beta\gamma\delta} a_\alpha^\dagger a_\beta^\dagger a_\gamma a_\delta \tag{27}$$

$$t_{\alpha\beta} = \int dx_1 \Psi_\alpha(x_1)\left(-\frac{\nabla_1^2}{2} + \sum_i \frac{Z_i}{r_{1i}}\right)\Psi_\beta(x_1) \tag{28}$$

$$u_{\alpha\beta\gamma\delta} = \int\int dx_1 dx_2 \Psi_\alpha^*(x_1)\Psi_\beta(x_1)\frac{1}{|r_{12}|}\Psi_\gamma^*(x_2)\Psi_\delta(x_2) \tag{29}$$

For LiH and BeH_2 perfect filling of the 1s orbitals in the basis where H_1 is diagonalized and using a transformation on the annhilation and creation operators we can write $H_1^d = \sum_{\alpha=1}^{M} \omega'_\alpha a_\alpha^{'\dagger} a'_\alpha$ and since the 1s states are effectively filled one can approximate them to not interact with the higher orbitals and so this effectively reduces the number of qubits required for mapping to 6 or 8 for LiH and BeH_2 respectively.

Due to these two orbitals being filled all those terms in the hamiltonian would essentially contribute to an energy shift for single fermionic terms and also modifies the two fermionic terms since any terms with $a'^{\dagger}_{\alpha} a'_{\alpha}$ with $\alpha \in \{1s\uparrow, 1s\downarrow\}$. We now map the H_2 hamiltonian is mapped first onto 4 qubits using a binary tree mapping. The M spin orbitals are listed by first listing $M/2$ spin up ones and $M/2$ spin down ones. Then Z Pauli operators are assigned on the basis of the total number of electrons where if Z_M has even parity of electrons it is assigned +1 and otherwise -1 and based on the value of mod(m,4) we can decide what parity to assign to $Z_{M/2}$ and if m is odd then this parity can be either +1 or -1 and it would not really affect anything and so we get a degeneracy. Using all this we can effectively map this for H_2, LiH and BeH_2 as effectively 2,4 and 6 qubits each with 2, 25 and 44 tensor product basis sets and 4,99, 164 Pauli terms respectively.
Now we have described the method of gradient descent however the measurements of expectation value of the hamiltonian is not done directly by measurement. We represent the hamiltonian as a weighted sum of T Pauli terms on N qubits once mapping is done

$$H = \sum_{\alpha=1}^{T} h_\alpha P_\alpha \tag{30}$$

Where each $P_\alpha \in \{X, Y, Z, I\}^{\otimes N}$ and so we write the following by measuring each α-th Pauli operator.

$$\langle H \rangle = \sum_{\alpha=1}^{T} h_\alpha \langle P_\alpha \rangle \tag{31}$$

$$\text{Var}[H] = \sum_{\alpha=1}^{T} h_\alpha^2 \langle \Delta P_\alpha^2 \rangle \tag{32}$$

These individual Pauli operators are measured by correlating measurement outcomes of single qubit disperse readouts in the Z basis. The issue however is that if one samples a large number of trial states there an be a significant overload in measurement.
To minimize these sampling overheads the Pauli operators are grouped in sets $s_1, s_2, \ldots, s_A$ which have terms that are diagonal in the same tensor product basis. It is shown (in [4]) using numerical simulations that making use of this grouping can offer better results without as much overhead as opposed to not grouping. Also in the experiments done assignment errors which would occur at readout were taken into account by running readout calibrations at every angle update and then correcting the sampling account using the calibrations. It must be noted that there would be an exponential loss by weight of a certain Pauli operator and so binary tree encoding for representation of H as in equation 30 is important to prevent exponential scaling.

4.3 Applying on Quantum Magnets

To demonstrate how the advantage of greater circuit depths is crucially dependent on the target Hamiltonian, the paper explores a four qubit Heisenberg model in the presence of an external magnetic field. The Hamiltonian is described for it as follows

$$H = J \sum_{\langle ij \rangle} (X_i X_j + Y_i Y_j + Z_i Z_j) + B \sum_i Z_i \tag{33}$$

Here $\langle ij \rangle$ indicates the nearest neighbour pairs, J is the strength of spin-spin interaction and B is the magnetic field along the Z direction. The VQE technique is used to solve for the ground state energy. At $J = 0$ the ground state is completely separable and one can obtain the best estimate for a circuit with $d = 0$ as depth since the state can be characterized purely by rotations. However as J is increased, the ground states start getting more entangled and one would require a $d = 2$ depth with some U_{ENT} in the circuit to get the best estimate.

4.4 Conclusion

The main motivation of this algorithm is that given a Hamiltonian mapping it will produce the state which would have the minimum energy. The impressive feat I believe is that they were able to work this out for BeH_2 which is a fairly large molecule. It must be noted that as per the results obtained, the convergence of the energy happens at a value which is at an error of around 0.015 hartree. Also the gradient descent approach brings a big issue if one were to try to descent in functions where there are multiple minimas which one can only hope to avoid by choosing good parameter sets since this would be dependent on whether the Hamiltonian can be mapped in such a way that uniform convergence is guaranteed. One can also draw various similarities to Hamiltonians and cost functions for machine learning due to the gradient descent approach and is in fact used in a quantum machine learning algorithm.

5 Configuration Interaction

This section aims to summarize the discussions in [8].

5.1 The fundamentals

Configuration interaction (CI) is a method to solve the non relativistic Schrödinger equation described in equation 8. We have invoked the Born-Oppenheimer approximation and so we have to only consider a basis of N particle functions if we have a N electron molecule. We will assume a complete basis set of orbitals as $\{\chi_i(x_i)\}$ and we expand any arbitrary N electron state as $\Phi(x_1, x_2, \ldots, x_N) = \sum_{ij\ldots N} b_{ij\ldots N}\chi_i(x_1)\chi_j(x_2)\ldots\chi_N(x_N)$.
Since this is a wavefunction describing electrons (which are fermions) we have the constraint on it being asymmetric under exchange between any two electrons. As shown in equation 9 we get this by writing them as determinants called as Slater determinants. However one must note that there is a complete set of all possible Slater determinants which account for essentially replacing any number of spin orbitals which are filled with the unfilled ones and our final wavefunction would be a superposition of all such combinations. Certain exchanges may hardly have contribution in representation but some are essential to the representation of the wavefunction. We can hence write the state as a superposition of these possible "excitations" as shown in the below equation.

$$|\Psi\rangle = c_0 |\Phi_0\rangle + \sum_{ra} c_a^r |\Phi_a^r\rangle + \sum_{r<s,a<b} c_{ab}^{rs} |\Phi_{ab}^{rs}\rangle + \sum_{r<s<t,a<b<c} c_{abc}^{rst} |\Phi_{abc}^{rst}\rangle + \ldots \tag{34}$$

Here $|\Phi_r^a\rangle$ is the Slater determinant formed by replacing spin orbital a in $|\Phi_0\rangle$ with spin orbital r. The CI method aims to find these coefficients. While this may seem similar to perturbation theory, perturbation theory would approach this by taking the $|\Phi_0\rangle$ as the dominant configuration and accordingly proceed and is sure to fail if the dominant configuration itself is not dominant.
FUll CI corresponds to solving the Schrödinger's equation exactly withing the space spanned by the specified one-electron basis. If the one-electron basis is complete then this is called complete CI. As one can imagine the time complexity for doing Full CI or even complete CI is quite high (more on this later). A much more doable approach would first truncate the CI space and then proceed for example CISD only makes use of single and doubly excited configurations. This approach does infact provide a fairly accurate picture by accounting for nearly 95% of the correlation in small molecules in equilibrium configurations.
We now define a quantity called the correlation energy as follows

$$E_{corr} = \varepsilon_0 - E_{HF}$$

Here E_{HF} is the energy in the Hartree Fock limit and the exact non relativistic energy of the system is ε_0. The Hartree Fock energy would always be above the actual energy as can be seen by applying the variational theorem for minimizing the functional below

$$\mathcal{L} = \langle\Psi| \hat{H} |\Psi\rangle - E(\langle\Psi|\Psi\rangle - 1) \tag{35}$$

On minimizing the above functional by setting $\delta\mathcal{L} = 0$ one reaches the following equation (repeated indices are summed over)

$$H_{ij}c_j = ES_{ij}c_j \tag{36}$$

Here $|\Psi\rangle = \sum_i c_i |\Phi_i\rangle$, $H_{ij} = \langle\Phi_i|\hat{H}|\Phi_j\rangle$ and $S_{ij} = \langle\Phi_i|\Phi_j\rangle$. For an orthonormal basis this reproduces the actual Heisenberg equation. Since all energies would be greater than the actual minimum (which should be ε_0) that shows $E_{HF} \geq \varepsilon_0$.
Another consequence of the variational theorem for CI is the convergence of the wavefunction. An approximate variational wavefunction will have energy approaching that of the exact energy ε_0 as the approximate wavefunction approaches the exact one. While one may think that the variational approach on minimizing energy may not lead us to a state that necessarily satisfies all properties of the actual wavefunction like dipole moment for example, for a sufficiently large basis the wavefunction also converges along with the energy. Since one can extract all properties correctly once we have the exact wavefunction we essentially have a proper convergence with a good enough basis however the other properties may not converge as quickly as the energy would.

5.2 Reducing the CI space

A key part to being able to do CI is after the space has been truncated using certain techniques.

5.2.1 Using symmetries in CI space

We first begin with which N electron basis functions are useful to include in the total CI space. If we can find a set of these basis functions which contribute nothing to the hamiltonian then we might as well not use them. So let's say we have two eigenfunctions for some operator $\hat{A}$ as $|\phi_1\rangle$ and $|\phi_2\rangle$ where they have different eigenvalues. If we have that $[\hat{A}, \hat{H}] = 0$, this means that $\langle\phi_2| \hat{H} |\phi_1\rangle = 0$ since they would be simultaneously diagonizable. This tells us that if we can find a basis function which is an eigenfunction of an operator that commutes with the hamiltonian, all eiegenfunctions of this operator which have a different eigenvalue can be excluded from the CI space.
For example we can pick the operator $\hat{S}^2$ of spin angular momentum and we know that it commutes with the hamiltonian. However the basis functions are generally not eigenfunctions of spin angular momentum but certain linear combinations of them (called configuration state functions or CSFs) are and so using this we can directly reach that contribution of any basis function with the wrong spin should be zero. We can extend this to ant kind of symmetry operations of point groups enabling us to dispose of any basis states with incorrect irreducible representations.

5.2.2 Classification using excitation level

Often the truncation of CI space is done by ignoring all excitations beyond a certain level the most common being just considering doubly-excited configurations (CISD). First we must note the slater-condon rules which are as follows for a single electron operator for some n body system $\hat{F} = sum_i \hat{f}(i)$

$$\langle\Phi_0| \hat{F} |\Phi_0\rangle = \sum_i \langle\phi_i| \hat{f} |\phi_i\rangle \tag{37}$$

$$\langle\Phi_0| \hat{F} |\Phi_m^a\rangle = \langle\phi_m| \hat{f} |\phi_a\rangle \tag{38}$$

$$\langle\Phi_0| \hat{F} |\Phi_{mn}^{ab}\rangle = 0 \tag{39}$$

For a double electron operator for a many body system $G = \sum_{i,j\neq i} \hat{g}(i,j)$ we have

$$\langle\Phi_0| \hat{G} |\Phi_0\rangle = \sum_{i,j\neq i} (\langle\phi_i\phi_j| \hat{g} |\phi_i\phi_j\rangle - \langle\phi_i\phi_j| \hat{g} |\phi_j\phi_i\rangle) \tag{40}$$

$$\langle\Phi_0| \hat{G} |\Phi_m^a\rangle = \sum_i (\langle\phi_m\phi_i| \hat{g} |\phi_a\phi_i\rangle - \langle\phi_m\phi_i| \hat{g} |\phi_i\phi_a\rangle) \tag{41}$$

$$\langle\Phi_0| \hat{G} |\Phi_{mn}^{ab}\rangle = \langle\phi_m\phi_n| \hat{g} |\phi_a\phi_b\rangle - \langle\phi_m\phi_n| \hat{g} |\phi_b\phi_a\rangle \tag{42}$$

$$\langle\Phi_0| \hat{G} |\Phi_{mno}^{abc}\rangle = 0 \tag{43}$$

Since the hamiltonian only has two body operators two states that differ in more than two excitations have no way to interact and so we can write the hamiltonian matrix as follows

$$\mathbf{H} = \begin{bmatrix} \langle\Phi_0| H |\Phi_0\rangle & & & & & \dots \\ 0 & \langle S| H |S\rangle & & & & \dots \\ \langle D| H |\Phi_0\rangle & \langle D| H |S\rangle & \langle D| H |D\rangle & & & \dots \\ 0 & \langle T| H |S\rangle & \langle T| H |D\rangle & \langle T| D |T\rangle & & \dots \\ 0 & 0 & \langle Q| H |D\rangle & \langle Q| H |T\rangle & \langle Q| H |Q\rangle & \dots \\ \vdots & \vdots & \vdots & \vdots & \vdots & \ddots \end{bmatrix} \tag{44}$$

Here $|S\rangle$, $|D\rangle$, $|T\rangle$ and $|Q\rangle$ represent block of single, doubly, triply and quadruply excited determinants respectively and the above matrix is hermitian and so only the lower diagonal terms have been written. This is essentially a block diagonal form of writing the matrix and all terms of $\langle S| H |\Phi_0\rangle = 0$ due to Brillouin's theorem since the reference wavefunction is obtained by the Hartree Fock method. While the other blocks need not be zero, they may be fairly sparse.
It can be seen that CISDTQ gives very high percentage of correlation energy for smaller molecules and generally will behave as the best option but will come at the cost of complexity. CISD gives about 95% correlation but only for equilibrium configurations and fails at stretched configurations. CISDT does not give much of an improvement over CISD and this shows that quadruple excitations are far more important than the triple excitations.

5.2.3 Size of CI space

Before commenting on the CI space size let us explore some different basis sets. We can define a certain orbital type called a Slater type orbital

$$\phi_{abc}^{STO} = N x^a y^b z^c e^{-\zeta r} \tag{45}$$

here $L = a + b + c$ and these orbitals are H atom like atleast for 1s but clearly are not pure spherical harmonics. They do give correct short range and long range behavior.
The next kind of orbitals which are easier to compute and used far more often are Gaussian type orbitals

$$\phi_{abc}^{GTO} = Nx^a y^b z^c e^{-\zeta r^2} \tag{46}$$

which again have $L = a + b + c$. These no longer are similar to the H atom like but are easier to compute due to the Gaussian form. Now since we are losing accuracy here there is another kind of orbital based on this called the contracted Gaussian type orbital which mimic an STO using GTOs in a linear sum. If n GTOs are used it is called as STO-nG and $\phi_{abc}^{CGTO} = N\sum_{i=1}^{n} x^a y^b z^c e^{-\zeta_i r^2}$. All these fall under minimal basis where one basis function (STO, GTO or CGTO) is used for the atomic orbital.
If one uses two basis functions for the atomic orbital it is called double-zeta, here specifically basis functions with different l values are mixed to get polarized functions and so is called double zeta polarization (DZP). This can be extended to any number of basis functions for the atomic orbital but beyond a point would surely be overkill. There is another example known as the Pople's split valence double zeta set 6-31G which uses 6 Gaussians for a CGTO core orbital and valence is ibed by two orbitals of 3 and 1 Gaussian respectively.
Now for getting the size of the CI space we will include spin symmetry and ignore spatial symmetry and apply Weyl's dimension formula. The dimension of CI space in CSFs is given by

$$D_{nNS}^{CSF} = \frac{2S+1}{n+1}\binom{n+1}{N/2-S}\binom{n+1}{N/2+S+1} \tag{47}$$

The dimension in determinants ignoring sparial symmetry is

$$D_{nNS}^{det} = \binom{n}{N/2-S}\binom{n}{N/2+S} \tag{48}$$

From the form of the above equations we can make out that computational complexity when working with this sized space would go in super-polynomial time. It's been seen that CISD scales as $\mathcal{O}(n^6)$ and CISDTQ scales as $\mathcal{O}(n^{10})$ where n is the number of orbitals. This is extended as $\mathcal{O}(n^{2m+2})$ where m is the number of excitations being taken account of. A proper proof for the scaling can be found in [gatech notes]. This shows that for full CI we have $\mathcal{O}(D_{nNS}^{det} N^2 n^2)$ which is clearly superpolynomial time.

5.2.4 Frozen-core approximation

The frozen core approximation is quite common in CI calculations. This essentially is to assume that all the lowest lying molecular orbitals have to be constrained to be doubly occupied. These are primarily the inner shell atomic orbitals which would be 1s for atoms lithium to neon and 1s, 2s, $2p_x$, $2p_y$, $2p_z$ for sodium to argon. This effectively decreases the size of the CI space quite significantly and we can effectively write the modified hamiltonian as follows

$$\hat{H}_0 = E_c + \sum_{i=1}^{N-N_c} \hat{h}_c(i) + \sum_{i>j}^{N-N_c} \frac{1}{r_{ij}} \tag{49}$$

Here the offset energy of E_c accounts for the doubly occupied orbitals which are now fixed and has the following expression

$$E_c = 2\sum_{i}^{n_c} h_{ii} + \sum_{ij}^{n_c} \{2(ii|jj) - (ij|ji)\} \tag{50}$$

And the operator $\hat{h}_c(i)$ is the one electron hamiltonian operator for electron i in the average filed produced by the N_c core electrons.

$$\hat{h}_c(i) = \hat{h}(i) + \sum_{j=1}^{n_c} \left\{2\hat{J}_j(i) - \hat{K}_j(i)\right\} \tag{51}$$

Here $\hat{J}_j(i)$ and $\hat{K}_j(i)$ represent the standard Coulomb and exchange operators respectively. We can also define a frozen core density matrix as $P_{\rho\sigma}^c = \sum_i^{n_c} C_\rho^i C_\sigma^i$ where C_ρ^i is the contribution of atomic orbital ρ to the molecular orbital i and with this we can rewrite

$$h_{\mu\nu}^c = h_{\mu\nu} + 2\sum_{\rho\sigma}(\rho\sigma|\mu\nu)P_{\rho\sigma}^c - \sum_{\rho\sigma}(\rho\mu|\nu\sigma)P_{\rho\sigma}^c \tag{52}$$

And with this the energy can be simplified to $E_c = \mathrm{Tr}(P^c h + P^c h^c)$. Similar to this approximation one can make an assumption that the highest lying virtual molecular orbitals are constrained to remain unoccupied in all configurations since they would be of higher energies but can only be valid for the very high lying orbitals.

5.3 Second Quantization

Here I will just list the notation used of second quantization in CI theory. Since we have fermions we get the following anticommutation relations for annihilation and creation operators.

$$\{a_j, a_i\} = a_j a_i + a_i a_j = 0 \tag{53}$$

$$\{a_j^\dagger, a_i^\dagger\} = a_j^\dagger a_i^\dagger + a_i^\dagger a_j^\dagger = 0 \tag{54}$$

$$\{a_i, a_j^\dagger\} = a_i a_j^\dagger + a_j^\dagger a_i = \delta_{ij} \tag{55}$$

We now define the one electron and two electron operations in this formalism using annihilation and creation operators.

$$\hat{O}_1 = \sum_{ij}^{2n} \langle i| \, h \, |j\rangle \, a_i^\dagger a_j \tag{56}$$

$$\hat{O}_2 = \frac{1}{2} \sum_{ijkl}^{2n} \langle ij| \, kl\rangle a_i^\dagger a_j^\dagger a_l a_k \tag{57}$$

Here we have used a shorthand notation of physicists which is $|i\rangle = |\phi_i\rangle$ and the two electron integral of $\int dx_1 dx_2 \phi_i^*(x_1)\phi_j^*(x_2)\phi_k(x_1)\phi_l(x_2) = \langle ij|kl\rangle$. All the summations sum over all the $2n$ spin orbitals. The hamiltonian can be written as

$$\hat{H} = \sum_{pq}^{2n} a_p^\dagger a_1 [p|h|q] + \frac{1}{2} \sum_{pqrs}^{2n} a_p^\dagger a_r^\dagger a_s a_q [pq|rs] \tag{58}$$

Here the square bracket representation is equivalent to the previously mentioned representation and is just the chemist's notation. We now define a shift operator as follows

$$\hat{E}_{ij} = a_{i\alpha}^\dagger a_{j\alpha} + a_{i\beta}^\dagger a_{j\beta} \tag{59}$$

This is isomorphic to the generators of the unitary group. One can simplify the hamiltonian after breaking it into the sum of a one electron operator and a two electron operator and then summing them after some simplification to get

$$\hat{H} = \sum_{pq}^{n} (p|h|q)\hat{E}_{pq} + \frac{1}{2} \sum_{pqrs}^{n} (pq|rs) \left(\hat{E}_{pq}\hat{E}_{rs} - \delta_{qr}\hat{E}_{ps} \right) \tag{60}$$

5.4 Determinant-Based CI & the algorithm

While CSFs clearly offer a reduced CI space, many modern algorithms make use of determinants instead since they offer certain computational advantages. An example of this is demonstrated in [5] where the Cooper-Nesbet method is used for performing the CI iteration with the coefficients being updated according to the formula

$$\delta c_i = \frac{r_i}{E - H_{ii}} \tag{61}$$

Where the r vector is defined as

$$r_i = \sum_j (H_{ij} - E\delta_{ij}) c_j \tag{62}$$

Handy realized that if determinants are used as basis functions and particularly can be expressed as alpha strings and beta strings, then H_{ij} can be computed efficiently.

5.4.1 Alpha and Beta strings

We define the alpha string as an ordered product of creation operators for spin orbitals with alpha spin and the beta string is defined similarly for the beta spin. For example if we have the slater determinant $|I\rangle = |\phi_{1\alpha}\phi_{2\alpha}\phi_{3\alpha}\phi_{1\beta}\phi_{2\beta}\phi_4\beta\rangle$, the alpha string for this would be $\alpha(I_\alpha) = a_{1\alpha}^\dagger a_{2\alpha}^\dagger a_{3\alpha}^\dagger$ and the beta string would be $\beta(I_\beta) = a_{1\beta}^\dagger a_{2\beta}^\dagger a_{4\beta}^\dagger$. The order of writing matters here since an exchange would result in a negative sign being introduced. To make a convention, the orbitals are listed in strictly increasing order and the beta string is placed to the right of the alpha string.
There are some advantages of using these strings. Direct CI methods require an index vector that points to a list of all the allowed excitations on the basis functions. Using he alpha and beta strings, this vector need not have the same

length as the CI vector and would infact be approximately the square root of the number of determinants. This results from the fact that alpha orbitals can only excite to alpha orbitals and this is similarly true for beta orbitals. An additional efficiency increase happens for calculation of $\langle\alpha(I_\alpha)\beta(I_\beta)|\,\hat{H}\,|\alpha(J_\alpha)\beta(I_\beta)\rangle$ since this integral is completely independent on the beta string.
The actual representation of alpha and beta strings is done using walks on a graph where they have a unique index or address obtained by adding the weights of the edges in the walk.

5.4.2 Restricted Active Space CI

The restricted active space (RAS) method calls for the partitioning of the one electron basis into four subsets. The first subset contains the core orbitals which are constrained to remain doubly occupied. The remaining three subsets are labelled as I, II and III and have a constraint set on them that I requires a minimum of p electrons and III can have a maximum of q electrons. The full CI can be obtained as a maximum limit of the RAS space. The RAS CI method depends on Handy's separation of determinants into alpha and beta strings. Using RAS CI the CI space is restricted by not allowing all alpha and beta strings and not allowing certain combinations too. Since N is fixed, the lengths of the alpha and beta strings n_α and n_β are constant too. While it would be possible to create a table of all allowed combinations of alpha and beta strings, one can make use of multiple graphs to get a more efficient approach. For example one can use a graph for all strings with no electrons in RAS III, one with one electron in III and one for two in III. The combinations of these graphs would now have restrictions as per the restrictions required on strings.

5.4.3 Olsen's Full CI

We now note our CI vector as $C(I_\alpha, I_\eta)$ and using the second quantized form of the hamiltonain we write the following

$$\sigma(I_\alpha, I_\beta) = \sum_{J_\alpha, J_\beta} \langle\beta(J_\beta)\alpha(J_\alpha)|\,\hat{H}\,|\alpha(I_\alpha)\beta(I_\beta)\rangle\, C(J_\alpha, J_\beta) \tag{63}$$

This above expression can be broken down into three parts such that $\sigma(I_\alpha, I_\beta) = \sigma_1(I_\alpha, I_\beta)+\sigma_2(I_\alpha, I_\beta)+\sigma_3(I_\alpha, I_\beta)$. Here σ_1 has no α operators and similarly σ_2 has no β operators. The remaining part is written as σ_3. The expression of σ_1 is written below and one can obtain the expression for σ_2 by just exchanging α and β in the below equation.

$$\begin{aligned}\sigma_1(I_\alpha, I_\beta) = \sum_{J_\beta}\sum_{kl}^{n} \langle\beta(J_\beta)|\,\hat{E}^\beta_{kl}\,|\beta(I_\beta)\rangle \left[h_{kl} - \frac{1}{2}\sum_{j}^{n}\langle kj|jl\rangle\right] C(I_\alpha, J_\beta) \\ +\frac{1}{2}\sum_{J_\beta}\sum_{ijkl}^{n} \langle\beta(J_\beta)|\,\hat{E}^\beta_{ij}\hat{E}^\beta_{kl}\,|\beta(I_\beta)\rangle\,\langle kj|jl\rangle C(I_\alpha, J_\beta)\end{aligned} \tag{64}$$

We finally get the following for σ_3

$$\sigma_3(I_\alpha, I_\beta) = \frac{1}{2}\sum_{J_\alpha, J_\beta}\sum_{ijkl}^{n} \langle\beta(J_\beta)|\,\hat{E}^\beta_{ij}\,|\beta(I_\beta)\rangle\,\langle\alpha(J_\alpha)|\,\hat{E}^\beta_{kl}\,|\alpha(I_\alpha)\rangle\,\langle kj|jl\rangle C(I_\alpha, J_\beta) \tag{65}$$

5.4.4 Full CI algorithm

Due to $\sigma_1(I_\alpha, I_\beta)$ being independent of I_α apart from the multiplication by factor of $C(I_\alpha, J_\beta)$ it is possible to vectorize it. We can obtain $\sigma_2(I_\alpha, I_\beta) = (-1)^S\sigma_1(I_\beta, I_\alpha)$ for $M_S = 0$ states but even otherwise due to them having the same expression except for exchange of α and β even that can be analogously vectorized. For vectorizing σ_3 a vectorized gather-scatter is used for addressing which is the same as just a map with indices for an-

other array. For $M_S = 0$ we have $\sigma_3^{ijkl}(I_\alpha, I_\beta) = (-1)^S \sigma_1^{klij}(I_\beta, I_\alpha)$ which we can use for a slight speedup.

Algorithm 1: Vectorized algorithm for σ_1

while ***loop*** *over* I_β **do**
  $F(J_\beta) = 0$ initialize;
  while ***loop*** *over* $\hat{E}_{kl}^\beta$ *from* $|\beta(I_\beta)\rangle$ **do**
    $|\beta(K_\beta)\rangle = \text{sgn}(kl)\hat{E}_{kl}^\beta |\beta(I_\beta)\rangle$;
    $F(K_\beta) += \text{sgn}(kl) h'_{kl}$;
    while ***loop*** *over* $\hat{E}_{ij}^\beta$ *from* $|\beta(K_\beta)\rangle$ **do**
      $|\beta(J_\beta)\rangle = \text{sgn}(ij)\hat{E}_{ij}^\beta |\beta(K_\beta)\rangle$;
      $F(K_\beta) += (1/2)\text{sgn}(kl)\text{sgn}(ij)(ij|kl)$;
    end
  end
  $\sigma_1(I_\alpha, I_\beta) = \sum_{J_\beta} F(J_\beta) C(I_\alpha, J_\beta)$ vectored over I_α;
end

Algorithm 2: Vectorized algorithm for σ_3

while ***loop*** *over* kl **do**
  set up $L(I)$, $R(I)$ and $\text{sgn}(I)$ defined below;
  $|\alpha[L(I)]\rangle = \hat{E}_{kl}^\alpha |\alpha[R(I)]\rangle \text{sgn}(I)$;
  $C'(I, J_\beta) = C[L(I), J_\beta]\text{sgn}(I)$ vectorized gather;
  while ***loop*** *over* I_β **do**
    while ***loop*** *over* $\hat{E}_{ij}^\beta$ *from* $|\beta(I_\beta)\rangle$ **do**
      $|\beta(J_\beta)\rangle = \text{sgn}(ij)\hat{E}_{ij}^\beta |\beta(I_\beta)\rangle$;
      $F(J_\beta) += \text{sgn}(ij)(ij|kl)$;
    end
    $V(I) = \sum_{J_\beta} F(J_\beta) C'(I, J_\beta)$ vectored over I;
    $\sigma_3[R(I), I_\beta] += V(I)$ vectorized scatter;
  end
end

5.5 Conclusion

We have exhaustively summarized some of the basics in CI theory in this section. The question now is whether one can actually modify the algorithm in some way so as to obtain a speed up in computational or space complexity while using a quantum computer. In [7] there is a description for quantum search using Grover's iterations on an unstructured database and this potentially offers quadratic speedup on any problem which requires a linear search as part of it. Another set of problems specifically the hidden subgroup problem also get speedups using quantum computers. The main approach remains in making use of parallelism in the calculations with an appropriate oracle and to be able to find a "faster CI" we would need to first find an efficient mapping to qubits, then see whether we can map the problem to something where we know a speedup exists. We have seen that FCI is actually used as a benchmark to verify approximate quantum algorithms like VQE or phase estimation and so if it is possible to speed up CI calculations with a quantum computer that potentially offers the best way to do quantum chemistry calculations.

6 Gate-free state preparation for fast variational quantum eigensolver simulations

This section aims to summarize [6]. Currently due to limitations of finite coherence times and gate errors, the number of gates that can be implemented on current devices are not high enough to accurately simulate strongly correlated molecules which require significant entanglement. In [6], an alternative implementation of VQE dubbed as `ctrl-VQE` is proposed which prepared states using a quantum control routine to variationally drive the Hartree-Fock state to the target full CI state and using this compute the energy of LiH with four transmons.

6.1 The Method

6.1.1 Variational Quantum Eigensolver

I have discussed VQE methods in more depth in section 4.1 which was summarized from [4]. We first would write the second electronic Hamiltonian into an equivalent form involving non local strings of Pauli spin operators $\hat{S}_i$.

$$\hat{H}^{\text{molecule}} = \sum_{pq} h_{pq}\hat{p}^\dagger\hat{q} + \frac{1}{2}\sum_{pqrs}\langle pq|rs\rangle\hat{p}^\dagger\hat{q}^\dagger\hat{s}\hat{r} \tag{66}$$

$$= \sum_i \hat{S}_i h_i \tag{67}$$

Here h_i is a sum of molecular one or two electron integrals and the $\hat{p}$ operators are fermionic annihilation operators. We can see that this is the same as eq:60. We can get the form of writing it in forms of strings of pauli operators using various transformations one example being the Jordan-Wigner transformation. The Jordan wigner transformation maps as follows from a fermionic annihilation operator q_p to string of pauli operations labelled here as $\tilde{q}_p$

$$q_p \mapsto \frac{1}{2}(X_p + \mathrm{i}Y_p)Z_1\cdots Z_{p-1} \tag{68}$$

$$= (|0\rangle\langle 1|)_p Z_1\cdots Z_{p-1} \tag{69}$$

$$=: \tilde{q}_p \tag{70}$$

The steps involved have been summarized in section 4.1.

6.1.2 Control Variational Quantum Eigensolver `ctrl-VQE`

The algorithm for this is quite similar to VQE but replaces the parameterized state preparation circuit with a parameterized laboratory. The standard procedure follows as described below

1. Map the hamiltonian to a qubit representation and compute the one and two electron integrals required for the same to define the objective (cost) function to minimize, being $\langle\hat{H}^{\text{molecule}}\rangle$
2. Define a fixed pulse representation (e.g. square pulses, sums of Gaussian pulses, etc.) and parametrize this chosen pulse representation and choose an initial set for them.
3. Choose the initial state for the qubit system. The HF state is usually a good choice for such problems.
4. Measure the objective (cost) function on the quantum device.
5. Using a classical optimization routine set the new parameters for the next measurement.
6. Repeat until convergence of desired threshold is met. If the chosen parametrized pulse can span the target Hilbert space, the optimal pulse would have found the minimum energy state.

A thing to note is that the pulse duration is taken as a hyperparameter which can be optimized in the outer-loop. Also unlike universal quantum computing algorithms this algorithm occurs at the hardware level and in this paper the well established transmon platform is used. The hamiltonian of the 1D device is as follows

$$\hat{H}_D = \sum_{k=1}^{N}\left(\omega_k\hat{a}_k^\dagger\hat{a}_k - \frac{\delta_k}{2}\hat{a}_k^\dagger\hat{a}_k^\dagger\hat{a}_k\hat{a}_k\right) + \sum_{\langle kl\rangle} g(\hat{a}_k^\dagger\hat{a}_l + \hat{a}_l^\dagger\hat{a}_k) \tag{71}$$

Here the summation over $\langle kl\rangle$ is over pairs of coupled qubits, $\hat{a}_k$ is the bosonic annihilator for the kth transmon, and ω_k, δ_k and g are resonant frequency, anharmonicity and constant coupling rate respectively. The results were found to not depend qualitatively on freqeuncy difference between qubits. The control hamiltonian has the following expression for a real valued drive $\Omega_k(t)$ applied on the device

$$\hat{H}_C = \sum_{k=1}^{N}\Omega_k(t)(e^{\iota\nu_k t}\hat{a}_k + e^{-\iota\nu_k t}\hat{a}_k^\dagger) \tag{72}$$

The total hamiltonian would now be the sum of $H = \hat{H}_D + \hat{H}_C$. In the interacting fram the final ansatz takes the form of $|\psi^{\text{trial}}(\Omega_n(t),\nu_n)\rangle = \mathcal{T}e^{-\iota\int_0^T dt\hat{H}_C(t,\Omega_n(t),\nu_n)}|\psi_0\rangle$. Here T is the total pulse time and $\mathcal{T}$ is the time ordering

operator. While the control hamiltonian above has only single qubit terms the device itself would have two qubit couplings with strength of g which create an entangling hamiltonian in the interacting frame

$$\hat{H}(t)_C = e^{\iota \hat{H}_D t} \hat{H}_C(t) e^{-\iota \hat{H}_D t} \tag{73}$$

This signifies that the coupling strength is what would be responsible to describe electron correlation in the target molecule. The final cost function to minimize is $E(\Omega_n(t), \nu_n) = \langle \psi^{\text{trial}} | \hat{H}^{\text{molecule}} | \psi^{\text{trial}} \rangle$ and the kets here can be either normalized or unnormalized as they would still minimize effectively the same.
When it comes to defining the pulses, parametrized square pulses are defined as follows

$$\Omega_k(t) = \begin{cases} c_1 & 0 \leq t < t_1 \\ c_2 & t_1 \leq t < t_2 \\ \vdots & \\ c_n & t_{n-1} \leq t < T \end{cases} \tag{74}$$

Here t_i are the switching times and c_i are the various amplitudes. Each transmon is also driven by a frequency modulation of form $\exp(\iota \nu_k t)$ where $|\omega_k - \nu_k| < 2\pi$ GHz. The parameters we have are hence c_i, t_i, ν_i. With N transmons and n square pulses there is a total of $2Nn$ paramteres to optimize and the routine used is 1-BFGS-b and hence we have a complexity of $\mathcal{O}(N^2 n^2)$ for updating parameters.
The STO-3G basis set was used throughout. The authors of [6] also published a python package `CtrlQ`

6.2 Results and discussion

6.2.1 Dissociation of diatomic molecules

Although being small molecules, HeH^+ and H_2 have served as general benchmarks for quantum algorithms in recent years. Since these are two orbital, two electron problems these can be mapped to four qubits using Jordan-Wigner transform (eq: 68-70) however using a parity mapping (described below) two qubits come out to be diagonal and so can be removed from consideration.

$$a_p \mapsto \frac{1}{2}(X_p Z_{p-1} + \mathrm{i} Y_p) X_{p+1} \cdots X_N \tag{75}$$

$$= \frac{1}{4}[(X_p + \mathrm{i} Y_p)(I + Z_{p-1}) - (X_p - \mathrm{i} Y_p)(I - Z_{p-1})] X_{p+1} \cdots X_N \tag{76}$$

$$= [(|0\rangle\langle 1|)_p (|0\rangle\langle 0|)_{p-1} - (|0\rangle\langle 1|)_p (|1\rangle\langle 1|)_{p-1}] X_{p+1} \cdots X_N \tag{77}$$

As H_2 dissociates, the HOMO-LUMO gap shrinks and so the mean field approximation does not remain very faithful hence HF state loses accuracy however HeH^+ in contrast gets better accuracy at higher bond distances. This is since it is the strongest acid (and interestingly the first molecule formed in the universe) and hence dissociation is a heterolytic deprotonation. The paper shows that `ctrl-VQE` reproduces the FCI bond dissociation curve of H_2 and HeH^+ with high accuracy.
For H_2 as bond dissociates the singlet ground state becomes degenerate with the lowest triplet state and hence there is a possibility of the superposition of them to form. To avoid this there can be a modification done to the objective function by adding a certain penalty to it giving us the following objective function

$$\langle H \rangle + \alpha(1 - || \, |\psi\rangle_s \, ||)^2 + \beta(\langle s \rangle - s_t)^2 \tag{78}$$

Here $|\psi\rangle_s$ is the state projected onto the qubit subspace and s is the total spin operator for our reduced space given by the operator below. For a singlet state $s_t = 0$. Also α and β are simply constants.

$$s = \begin{pmatrix} 1 & 0 & 0 & -1 \\ 0 & 0 & 0 & 0 \\ 0 & 0 & 0 & 0 \\ -1 & 0 & 0 & 1 \end{pmatrix} \tag{79}$$

This essentially helps us in tackling the leakage issues due to degenerate states which would be outside of the qubit subspace.

6.2.2 Leakages and pulse duration

Molecules which are strongly correlated tend to be difficult to simulate using VQE since they generally require higher depth of circuits which brings up more noise. Analogously in `ctrl-VQE` longer pulses are expected for such kinds of

molecules as entanglement cannot be created instantly.
What we deem as leakage here is the amount of the population that lies outside of the basis states. As per the results of [6] this seemed to increase with evolution time. However the actual leakage amount does also change depending on the total pulse time T. Another thing to note is that the convergence of the molecular energy for both the example molecules is not monotonically decreasing but rather initially increases and then proceeds to rapidly decrease.

6.2.3 Comparison with Circuit Compilation Techniques

To execute normal gate based VQE, the gates are compiled into sequences of analog control pulses using a certain look-up table to map each gate to some analog pulse. As such this compilation is near instantaneous and well suited for VQE due to numerous iterations being performed. However this may result in very a long pulse duration which could be avoided by using optimized compilation techniques.
One such example being the GRAPE compilation technique which employs an optimal control routine which compiles to machine-level sequences of analog pulses. This however is quite costly since GRAPE updates time-discrete pulses using gradients hence is impractical for VQE despite possibly offering a 5-fold improvement.
One may see that GRAPE does seem similar to `ctrl-VQE` in the lines that both aim to generate a pulse which is equivalent to a certain circuit and involves updating parameters. However there is a fundamental difference in terms of the fact that GRAPE is a compilation technique for a certain already present circuit whereas while there is some circuit that is represented by a `ctrl-VQE` pulse there is no reference to such a circuit.
Now one can be sure that whatever analog pulse we do reach at in the end of `ctrl-VQE` has some unitary representation and this unitary can naturally be transpiled or decomposed to a normal quantum circuit. The paper made use of the KAK decomposition technique along with transpilation. Interestingly the pulse durations of the KAK decomposed circuit using the normal mapping came out as 1202 ns and transpiling gave 825 ns in stark contrast to the original `ctrl-VQE` pulse being 9 ns for the H_2 molecule at a bond distance of 0.075 nm. This indicates how much of the circuit depth is actually unnecessary to some extent.

6.2.4 Adaptive update of pulse parametrization

A common issue in problems which involve updating parameters is the possibility of over-paraemetrizing the system. The paper proposes a scheme for adaptively updating the pulse to prevent a large number of parameters where instead of a fixed number of time divisions, the number of time segments is increased as the algorithm progresses.

1. Initialize a square pulse with $n = 1$ time segment.
2. Divide the pulse at some randomly chosen time so $n = 2$ now.
3. Perform the pulse optimization.
4. Divide the largest time segment into two using a randomly chosen time making number of segments as $n+1$.
5. Perform pulse optimization on the new pulse.
6. Repeat 4. and 5. till the wanted convergence is reached.

The total number of parameters to optimize would be $N(n+1)$ since irrespective of pulse shape only a single driving frequency is used. The amplitudes are constrained to stay between ± 40 MHz and the frequencies to be $\omega_k \pm 3\pi$ GHz. This adoptive strategy was tried on H_2, HeH^+ and LiH with a total duration of 9, 9, 40 ns respectively. Chemical accuracy (energy error smaller than 1 kcal/mol) was achieved for the first two with simply one time segment but required three for LiH.

6.3 Conclusion

The paper [6] offers a modified VQE which it successfully showed to quite accurately reproduce the full CI values of H_2, HeH^+ and even LiH with a modified version of itself. The results demonstrate that even with relatively modest number of parameters convergence in energy can be achieved as the problem size is increased. There is an impressive improvement over pulse durations in comparison to an actual VQE but it must be noted that this is a hardware based algorithm hence is not universal. Another point to note is that pulse shapes (which were square here for the most part) is another parameter which can be fine tuned and have more sophisticated constraints. Larger systems still are not explored through this method and would definitely require larger pulse duration to be able to describe stronger correlations.

References

[1] Frank Arute et al. "Hartree-Fock on a superconducting qubit quantum computer". In: *Science* 369.6507 (2020), pp. 1084–1089. ISSN: 0036-8075. DOI: 10.1126/science.abb9811. eprint: https://science.sciencemag.org/content/369/6507/1084.full.pdf. URL: https://science.sciencemag.org/content/369/6507/1084.

[2] Jiangfeng Du et al. "NMR Implementation of a Molecular Hydrogen Quantum Simulation with Adiabatic State Preparation". In: *Phys. Rev. Lett.* 104 (3 Jan. 2010), p. 030502. DOI: 10.1103/PhysRevLett.104.030502. URL: https://link.aps.org/doi/10.1103/PhysRevLett.104.030502.

[3] I. M. Georgescu, S. Ashhab, and Franco Nori. "Quantum simulation". In: *Rev. Mod. Phys.* 86 (1 Mar. 2014), pp. 153–185. DOI: 10.1103/RevModPhys.86.153. URL: https://link.aps.org/doi/10.1103/RevModPhys.86.153.

[4] Abhinav Kandala et al. "Hardware-efficient variational quantum eigensolver for small molecules and quantum magnets". In: *Nature* 549.7671 (Sept. 2017), pp. 242–246. ISSN: 1476-4687. DOI: 10.1038/nature23879. URL: http://dx.doi.org/10.1038/nature23879.

[5] Peter J. Knowles and Nicholas C. Handy. "A determinant based full configuration interaction program". In: *Computer Physics Communications* 54.1 (1989), pp. 75–83. ISSN: 0010-4655. DOI: https://doi.org/10.1016/0010-4655(89)90033-7. URL: https://www.sciencedirect.com/science/article/pii/0010465589900337.

[6] Oinam Romesh Meitei et al. *Gate-free state preparation for fast variational quantum eigensolver simulations: ctrl-VQE*. 2021. arXiv: 2008.04302 [quant-ph].

[7] Michael A. Nielsen and Isaac L. Chuang. *Quantum Computation and Quantum Information: 10th Anniversary Edition*. 10th. USA: Cambridge University Press, 2011. ISBN: 1107002176.

[8] C. Sherrill. "An Introduction to Configuration Interaction Theory". In: 1995.